An unusual pH-independent and metal-ion-independent mechanism for hairpin ribozyme catalysis

Stephen Nesbitt*, Lisa A Hegg† and Martha J Fedor*

Background: Hairpin ribozymes (RNA enzymes) catalyze the same chemical reaction as ribonuclease A and yet RNAs do not usually have functional groups analogous to the catalytically essential histidine and lysine sidechains of protein ribonucleases. Some RNA enzymes appear to recruit metal ions to act as Lewis acids in charge stabilization and metal-bound hydroxide for general base catalysis, but it has been reported that the hairpin ribozyme functions in the presence of metal ion chelators. This led us to investigate whether the hairpin ribozyme exploits a metal-ion-independent catalytic strategy.

Results: Substitution of sulfur for nonbridging oxygens of the reactive phosphate of the hairpin ribozyme has small, stereospecific and metal-ion-independent effects on cleavage and ligation mediated by this ribozyme. Cobalt hexammine, an exchange-inert metal complex, supports full hairpin ribozyme activity, and the ribozyme's catalytic rate constants display only a shallow dependence on pH.

Conclusions: Direct metal ion coordination to phosphate oxygens is not essential for hairpin ribozyme catalysis and metal-bound hydroxide does not serve as the general base in this catalysis. Several models might account for the unusual pH and metal ion independence: hairpin cleavage and ligation might be limited by a slow conformational change; a pH-independent or metal-cation-independent chemical step, such as breaking the 5′ oxygen–phosphorus bond, might be rate determining; or finally, functional groups within the ribozyme might participate directly in catalytic chemistry. Whichever the case, the hairpin ribozyme appears to employ a unique strategy for RNA catalysis.

Address: Department of Biochemistry and Molecular Biology, University of Massachusetts Medical Center, 55 Lake Avenue North, Worcester, MA 01655, USA.

Present addresses: *The Skaggs Institute for Chemical Biology, The Scripps Research Institute, 10550 North Torrey Pines Road, La Jolla, CA 92037, USA. †SmithKline Beecham, 1250 South Collegeville Road, Collegeville, PA 19420, USA.

Correspondence: Martha J Fedor
E-mail: mfedor@scripps.edu

Key words: cobalt hexammine, hairpin ribozyme, phosphorothioates, RNA catalysis

Received: **19 June 1997**
Accepted: **22 July 1997**

Chemistry & Biology August 1997, 4:619–630
http://biomednet.com/elecref/1074552100400619

Introduction

The hairpin ribozyme, along with the hammerhead, axehead and *Neurospora* VS catalytic RNAs, belongs to the family of small RNA endonucleases that reversibly cleave phosphodiesters of RNA substrates to generate 5′ hydroxyl and 2′,3′-cyclic phosphate termini (for review, see [1,2]). Found in the negative strand of the genome of the satellite RNA of tobacco ringspot virus [(–)sTRSV], hairpin-ribozyme-catalyzed self-cleavage and ligation reactions are believed to be responsible for processing intermediates in rolling circle replication [3].

A hairpin secondary structure model composed of two pairs of helix–loop–helix segments [4] is supported by truncation, mutagenesis, primer extension, phylogenetic comparison, *in vitro* selection, cross-linking, and chemical protection studies (reviewed in [5]). The sequence of most helical regions can vary without loss of activity, while mutations of most unpaired nucleotides impair activity. A symmetrical internal loop in the base of the hairpin stem contains the reactive phosphodiester. The two helix–loop–helix segments are thought to adopt a non-coaxial structure and to associate through additional tertiary interactions [6]. Although the hairpin domain assembles from sequences within a single RNA *in vivo*, separate ribozyme and substrate RNAs can combine through complementary base pairing to assemble an active ribozyme [4]. Intermolecular ribozyme configurations facilitate application of conventional enzymological methods to studies of catalytic mechanisms [7] and the design of ribozymes for antisense applications [8].

The cleavage mechanism of small self-cleaving RNAs involves deprotonation of the 2′ hydroxyl and in-line nucleophilic attack of the resulting 2′ oxyanion on the adjacent phosphorus. A trigonal bipyramidal transition state is generated in which five oxygens transiently bond to phosphorus (Figure 1, reviewed in [1]). Breaking of the 5′ oxygen–phosphorus bond is accompanied by protonation of the 5′ oxyanion leaving group. Ligation is a simple reversal of the cleavage reaction. The same reaction is catalyzed by ribonuclease A and other degradative ribonucleases and also occurs during nonenzymatic alkaline hydrolysis of RNA. In the catalytic mechanism of RNase A, an imidazole of a histidine residue, acting as a general base, removes a proton from the 2′ hydroxyl. A positively

Figure 1

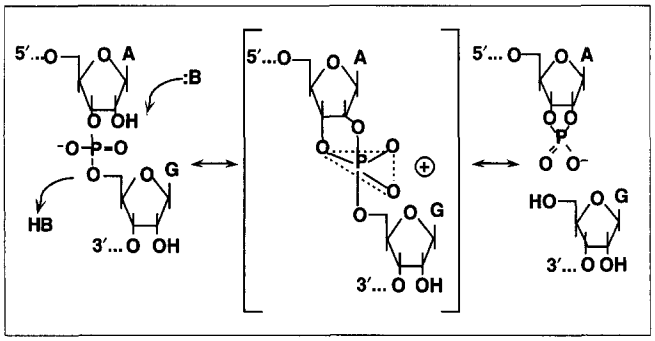

The mechanism of catalysis by self-cleaving RNAs. In the cleavage mechanism, the 2′ hydroxyl is deprotonated, leading to nucleophilic attack by the resultant 2′ oxyanion on the adjacent phosphorus. A trigonal bipyramidal transition state is generated, in which five oxygens transiently bond to phosphorus. Breaking of the 5′ oxygen–phosphorus bond is accompanied by protonation of the 5′ oxyanion leaving group. The ligation is simply the reversal of the cleavage reaction. B, base; A, adenosine; G, guanosine.

charged ε amino group of a lysine residue is positioned in the RNase A active site to counteract developing negative charge as the 2′ oxyanion attacks phosphorus. Protonation of the 5′ oxyanion leaving group by a histidine imidazolium, acting as a general acid, accompanies the breaking of the 5′ oxygen–phosphorus bond [9,10].

The dilemma for RNAs catalyzing proton transfer reactions is that RNA functional groups, at least in free nucleosides, have pK_a (pK_a is the log of the acid dissociation constant) values far outside the neutral range and are, therefore, not well-suited to serve as general acid–base catalysts at neutral pH. Furthermore, no ribonucleoside functional groups are positively charged at neutral pH to stabilize negative charge in the transition state. RNA enzymes are believed to solve this dilemma by recruiting metal ion cofactors to act as Lewis acids in charge stabilization and hydrated metal ions to act as general acid–base catalysts in proton transfer [11–14]. All RNA enzymes seem to require metal ions. Because all RNA enzymes are likely to require counterions to stabilize folded structures, a metal ion requirement for activity does not necessarily implicate metals in the catalytic chemistry. Changes in divalent metal ion specificity that accompany substitution of sulfur for phosphate oxygens have implicated direct coordination of metal cations to phosphate oxygens for the hammerhead ribozyme and the *Tetrahymena* self-splicing ribozyme [15,16]. 'Hard' metal ions such as Mg^{2+} bind to oxygen ligands well, but bind to sulfur ligands poorly, while 'soft' metal ions such as Mn^{2+} bind to oxygen ligands and sulfur ligands with similar affinities [17,18]. Substitution of sulfur for the *pro-R*p oxygen of the reactive phosphate inhibits hammerhead cleavage in buffers containing Mg^{2+} but not in buffers containing Mn^{2+}, implicating direct metal cation coordination to the nonbridging *pro-R*p oxygen in the hammerhead transition state [15,19,20]. The *Tetrahymena* ribozyme cleaves phosphodiesters in a mechanistically distinct reaction that generates 3′ hydroxyl and 5′ phosphate termini. In the *Tetrahymena* reaction, substitution of the bridging 3′ oxygen at the cleavage site with sulfur inhibits cleavage in buffers containing Mg^{2+} but not in buffers containing Mn^{2+} or Zn^{2+}, implicating metal cation coordination in the stabilization of the negative charge on the 3′ oxyanion leaving group [16].

Additional evidence for a catalytic role for metal ions comes from the correspondence between cleavage rates and the titration of metal-bound water molecules as a function of pH to promote general base catalysis in hammerhead cleavage [21]. Comparison of hammerhead reaction rates in buffers with different metal cations shows that pH-rate profiles shift in accordance with the pK_a of the hydrated metal ion included in the reaction buffer, and cleavage displays a log-linear dependence on pH. This correlation between cleavage rates and metal-hydroxide concentrations is consistent with the metal hydroxide acting as a general base catalyst to deprotonate the 2′ hydroxyl in a reaction limited by the availability of the 2′ oxyanion nucleophile.

The hairpin ribozyme appears to exploit a distinct catalytic strategy, one that does not require metal-bound water complexes or direct coordination of metal cations to phosphate oxygens. While no hammerhead ribozyme activity is observed in the absence of divalent metal cations, even when alternative counterions are available to stabilize hammerhead structure [21], hairpin ribozyme catalysis has been detected in buffers containing metal ion chelators, although at significantly reduced levels [22,23]. Substitution of the *pro-R*p oxygen of hairpin substrates with sulfur had only small effects on hairpin cleavage in buffers with Mg^{2+} [23,24]. This result argues against direct coordination of Mg^{2+} to the *pro-R*p oxygen because Mg^{2+} binds to sulfur poorly. Furthermore, the hairpin ribozyme remains active in buffers containing cobalt(III)hexammine in place of $MgCl_2$ (A. Hampel, personal communication). The amine ligands of cobalt hexammine are kinetically stable [25] and do not exchange to allow direct coordination of Co^{3+} with phosphate oxygens or with water molecules to generate metal hydroxides capable of general base catalysis. We have confirmed and extended these results by assessing the effects of *R*p and *S*p phosphorothioate substitutions on hairpin-catalyzed cleavage and ligation rate constants and the pH- and metal-ion-dependence of these effects.

Results and discussion

The effects of phosphorothioate substitutions on hairpin ribozyme cleavage rate constants

The ribozyme sequence used to measure cleavage kinetics (Figure 2a) is derived from the minimal self-cleaving

domain of (–)sTRSV [4]. The cleavage substrate has an unpaired 5′ terminal cytosine, a modification previously found to simplify kinetic analyses by minimizing non-productive complex formation [7]. Short substrates were chosen for determination of cleavage rate constants to ensure that cleavage was driven by rapid dissociation and dilution of cleavage products, so that observed cleavage rates monitor the rate-determining step in cleavage and not the approach to an equilibrium between cleavage and ligation or product dissociation steps [7].

Hairpin substrate RNAs with sulfur substituted for *pro-R*p or *pro-S*p nonbridging oxygens of the reactive phosphate (Figure 2b) were prepared by sulfurization during chemical synthesis, separated by reverse phase high pressure liquid chromatography (HPLC) [20] and identified by digestion with stereospecific specific snake venom and P1 nucleases. Both the *R*p and *S*p diastereomers reacted almost completely and with first order kinetics, confirming the homogeneity of substrate RNA preparations (data not shown).

The cleavage rate constant was fourfold lower for substrate with an *R*p phosphorothioate than for substrate with normal phosphate in buffer with 10 mM $MgCl_2$ (Figure 3a, Table 1). The modest inhibition of cleavage by an *R*p sulfur substitution is consistent with the previously reported effect of an *R*p phosphorothioate on hairpin activity [23,24]. Because *pro-R*p and *pro-S*p oxygens are very close in space, a small difference in active-site geometry between hammerhead and hairpin ribozymes might change the stereospecificity of a large 'thio effect'. The cleavage rate constant for substrate with an *S*p phosphorothioate was, however, slightly higher than for substrate with normal phosphate. Thus, for hairpin substrates, neither diastereomer gives rise to a thio effect of the same order as the > 100-fold inhibition reported for hammerhead cleavage of *R*p phosphorothioate substrates in buffers with 10 mM $MgCl_2$ [15].

It is important to rule out the possibility that contamination of $MgCl_2$ buffers with thiophilic metal ions able to coordinate phosphorothioates directly could account for the high reactivity of sulfur-substituted hairpin substrates. Addition of 1 mM diethyldithiocarbamate, a strong thiophilic metal ion chelator, produced no change in cleavage rate constants for normal or sulfur-substituted substrates. Thus, the small effects of *R*p and *S*p thio substitutions on hairpin cleavage in $MgCl_2$ buffers suggests that direct coordination of metal cations to either of the nonbridging phosphate oxygens is not essential for hairpin ribozyme catalysis.

The difference in thio effects between hairpin and hammerhead cleavage could arise from differences in kinetic mechanisms rather than differences between the two ribozymes in metal ion coordination. A large thio effect on hairpin catalytic chemistry could be underestimated if the chemical step is only partially rate-determining in the hairpin mechanism and a different step, such as a slow conformational change, also limits observed cleavage rates. If the small thio effect on hairpin cleavage reflects the loss of direct Mg^{2+} coordination, replacing Mg^{2+} with Mn^{2+}, which binds sulfur well, should restore full activity. The relative effects of *R*p and *S*p thio substitutions on hairpin cleavage were, however, virtually the same in buffers with $MgCl_2$ or $MnCl_2$ (Figure 3b, Table 1).

Figure 2

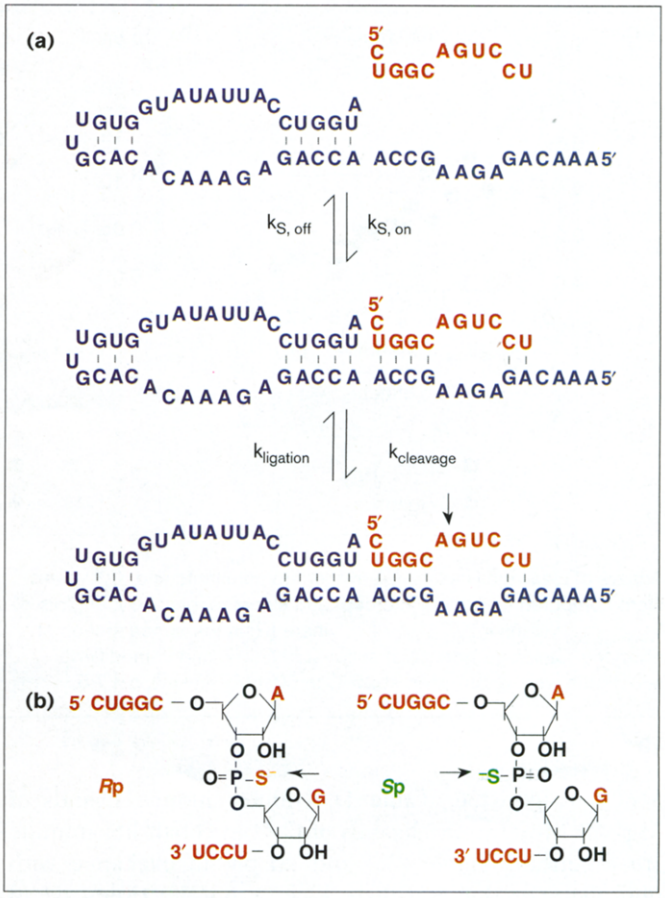

Analyzing the effects of sulfur substitutions of nonbridging oxygens on hairpin ribozyme cleavage activity. **(a)** Sequences used for analysis of cleavage kinetics. Trace amounts of 5′ ^{32}P-labeled substrate (red) were combined with various excess concentrations of hairpin ribozyme (blue) and the appearance of 5′ cleavage product (P^1; the arrow indicates the point of cleavage) was monitored over time. The choice of a small substrate ensures that cleavage is driven by rapid dissociation and dilution of cleavage products that bind the ribozyme with low affinity. **(b)** Hairpin substrates with thiophosphate substitutions at the reactive phosphate. The two diastereomer substitutions, *R* and *S*, that give P^1 and P^2, respectively, are shown.

Cobalt hexammine supports hairpin ribozyme catalysis

Similar small, stereospecific thio effects on hairpin cleavage are seen in buffers with $Co(NH_3)_6Cl_3$ in place of $MgCl_2$ or

Figure 3

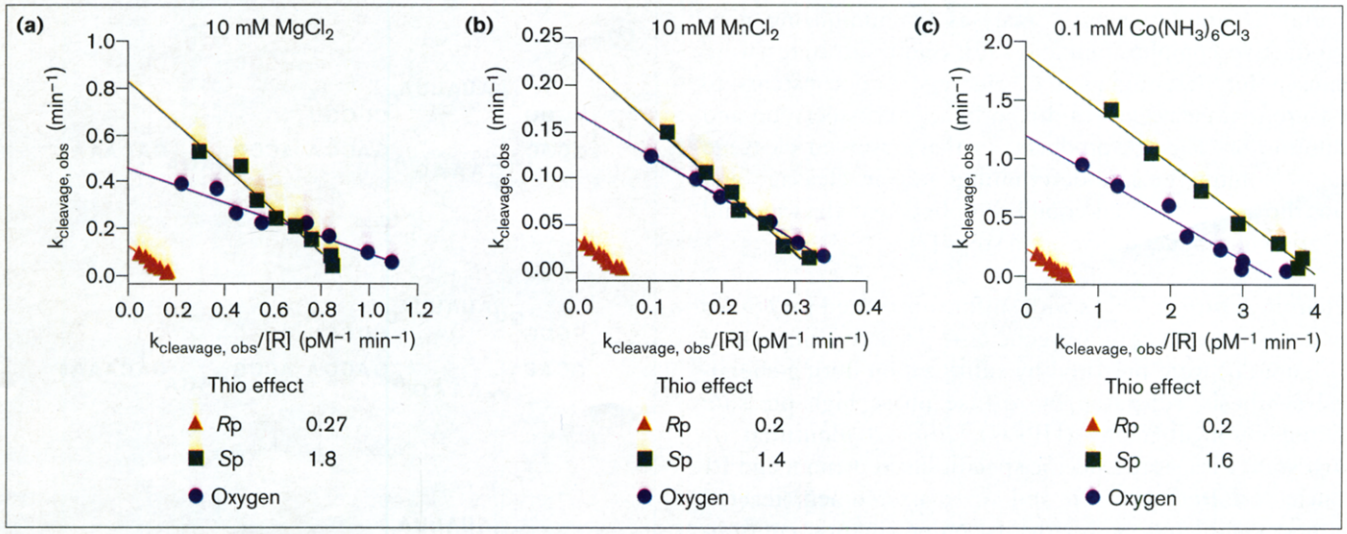

Assays of cleavage kinetics. Cleavage rate constants and K_M^S values were computed from the y intercept and slope, respectively, of plots of $k_{cleavage, obs}$ versus $k_{cleavage, obs}$ / [R], where [R] is the concentration of ribozyme. Cleavage kinetics of sulfur-substituted and unmodified substrates were determined at 25°C in 50 mM Tris-HCl, pH 7.5, 0.1 mM EDTA with **(a)** 10 mM $MgCl_2$, **(b)** 10 mM $MnCl_2$, or **(c)** 0.1 mM $Co(NH_3)_6Cl_3$. The 'thio effect' is $k_{cleavage, S}$ / $k_{cleavage, O}$ (S and O indicate sulfur and oxygen substituents, respectively). K_M^S, Michaelis constant for substrate; $k_{cleavage, obs}$, observed rate of cleavage.

$MnCl_2$ (Figure 3c, Table 1). Unlike chloride ligands of Mg^{2+} or Mn^{2+}, amine ligands of Co^{3+} in cobalt hexammine are kinetically stable [25] and unable to exchange with phosphate or thiophosphate ligands on the timescale of cleavage reactions. Thus, the ability of cobalt hexammine to support cleavage activity argues against a role for direct metal cation coordination to nonbridging phosphate oxygens, or any other ligands, in hairpin catalysis.

Despite the inability of Co^{3+} in cobalt hexammine to coordinate phosphate ligands directly, $Co(NH_3)_6Cl_3$ was particularly effective in promoting hairpin ribozyme catalysis compared to $MgCl_2$ (Figure 4). Half-maximal cleavage rate constants were observed in buffers with 0.1 mM $Co(NH_3)_6Cl_3$, while 100-fold higher concentrations of $MgCl_2$ were required to support the same level of activity. This difference in the metal ion concentration-dependence of hairpin cleavage in $Co(NH_3)_6Cl_3$ and $MgCl_2$ buffers was far greater than the twofold difference in ionic strength between $Co(NH_3)_6Cl_3$ and $MgCl_2$ solutions of the same molarity. This low $Co(NH_3)_6Cl_3$ concentration-dependence would not be expected if the ability of $Co(NH_3)_6Cl_3$ buffers to support hairpin catalysis could be explained by the presence of trace contaminants.

A number of control experiments were carried out to evaluate whether hairpin cleavage activity observed in $Co(NH_3)_6Cl_3$ buffers results from contaminating metal ions capable of direct phosphate coordination. No change in cleavage kinetics of sulfur-substituted or unmodified

Table 1

Cleavage kinetics of normal and phosphorothioate-substituted RNAs.

	10 mM $MgCl_2$			10 mM $MnCl_2$			0.1 mM $Co(NH_3)_6Cl_3$		
Linkage	$k_{cleavage}$ (min^{-1})	K_M^S (μM)	$\frac{k_{cleavage, S}}{k_{cleavage, O}}$	$k_{cleavage}$ (min^{-1})	K_M^S (μM)	$\frac{k_{cleavage, S}}{k_{cleavage, O}}$	$k_{cleavage}$ (min^{-1})	K_M^S (μM)	$\frac{k_{cleavage, S}}{k_{cleavage, O}}$
Phosphate	0.45	0.35		0.17	0.45		1.2	0.36	
Rp phosphorothioate	0.12	0.69	0.27	0.034	0.50	0.20	0.23	0.41	0.2
Sp phosphorothioate	0.82	0.89	1.8	0.23	0.69	1.4	1.9	0.47	1.6

$k_{cleavage}$, cleavage rate constant; K_M^S, Michaelis constant for substrate; $k_{cleavage, S}$ and $k_{cleavage, O}$ are cleavage rate constants for sulfur-substituted and unmodified substrates, respectively; $k_{cleavage, S}$ / $k_{cleavage, O}$, 'thio effect'.

Figure 4

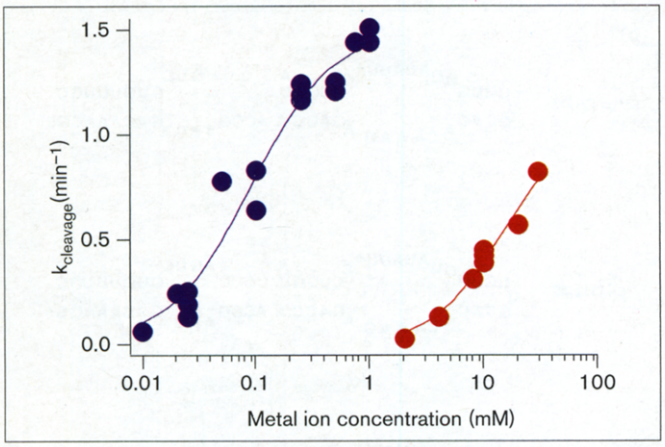

The dependence of hairpin cleavage rate constants on metal ion concentration. Cleavage rate constants for unmodified hairpin substrates were determined at 25°C in 50 mM Tris-HCl, pH 7.5, 0.1 mM EDTA, with varying concentrations of $MgCl_2$ (red) or $Co(NH_3)_6Cl_3$ (blue), as described in the legends to Figures 2 and 3. Lines represent fits to the cooperative binding equation:

$$k_{cleavage,\ obs} = k_{cleavage}\frac{[Me]^n}{[Me]^n + K_D^{Me}} \quad (5)$$

where K_D^{Me} is the dissociation constant for a given metal (Me), giving $K_D^{Mg} = 13$ mM and $K_D^{Co} = 0.1$ mM. Best fits were obtained with $n = 1.5$ for $MgCl_2$ and $n = 1.2$ for $Co(NH_3)_6Cl_3$.

substrate RNAs occurs when the concentration of EDTA in reaction buffers is increased from 0.1 mM to 1 mM, when buffer and RNA solutions are extracted with the strong chelator diphenylthiocarbazone [26], or when reaction buffers contain 1 mM diethyldithiocarbamate (a strong thiophilic metal ion chelator) in addition to 1 mM EDTA. Because the cobalt hexammine complex is thermodynamically unstable, despite its kinetic stability, cobalt hexammine solutions might produce degradation products over time that are responsible for promoting catalysis. Periodic monitoring of $Co(NH_3)_6Cl_3$ stock solutions over several months, however, revealed no changes in absorption spectra that might indicate accumulation of degradation products and no change in the ability of $Co(NH_3)_6Cl_3$ buffers to support catalysis. Finally, the R9/S9 hammerhead [27] showed no detectable cleavage activity in reaction buffers with $Co(NH_3)_6Cl_3$ included as the only metal cation (data not shown). Evidently, the ability of cobalt hexammine to promote activity is a unique feature of hairpin catalysis that argues against any requirement for metal ions capable of direct coordination to RNA functional groups.

The effects of phosphorothioate substitutions on ligation rate constants and the internal equilibrium between cleavage and ligation

Sulfur substitutions also produce small, stereospecific effects on hairpin-catalyzed ligation (Figure 5, Table 2). Consistent with the inversion of configuration that accompanies cleavage and ligation (Figure 5a), 2′,3′-cyclic thiophosphate with sulfur in the *R*p configuration ligates faster than thiophosphate with sulfur in the *S*p configuration. In 10 mM $MgCl_2$, the ligation rate constant for a 2′,3′-cyclic thiophosphate with sulfur in the *S*p configuration is ~8-fold lower than for an *R*p phosphorothioate and ~13-fold slower than for normal 2′,3′-cyclic phosphates (Figure 5c). Ligation rate constant measurements can be subject to considerable error, particularly when the difference between cleavage and ligation rate constants is small (see the Materials and methods section). The relative efficiency of *R*p and *S*p thiophosphate ligation remained at least qualitatively the same in $MnCl_2$ and $Co(NH_3)_6Cl_3$ buffers (Figure 5d,e), despite apparent variation in the magnitude of the thio effects.

Ligation and cleavage rate constants can be compared to assess the internal equilibrium ($K_{eq,\ int} = k_{ligation}/k_{cleavage}$). The $K_{eq,\ int}$ value of 4.5, calculated from phosphodiester cleavage and 2′,3′-cyclic phosphate ligation rate constants, is in reasonable agreement with the tenfold preference for ligation over cleavage reported previously for hairpin ribozymes [7]. For both *R*p and *S*p thiophosphate substitutions, however, $K_{eq,\ int}$ values were only slightly greater than 1 in $MgCl_2$ buffer. The considerable error inherent in comparisons of small differences in rate constants measured in independent assays limits the accuracy of $K_{eq,\ int}$ values calculated in this way. Qualitatively, however, sulfur in either an *R*p or an *S*p configuration appeared to shift the internal equilibrium towards cleavage.

An independent measure of the internal equilibrium for substrates with phosphates and thiophosphates at the cleavage site can be obtained from the relative amounts of substrate and product at equilibrium. The fraction of substrate formed at saturating concentrations, when all substrate and product is ribozyme bound, was extrapolated from the endpoints of ligation reactions carried out over a range of concentrations (Figure 6).

Two effects of phosphorothioate substitutions can be seen. First, *S*p and *R*p 2′,3′-cyclic thiophosphate substitutions produce a shift in the equilibrium towards cleavage, regardless of the metal ion present in reaction buffers. Second, a stereospecific effect of thio substitutions is seen in $Co(NH_3)_6Cl_3$ buffer, with the *S*p 2′,3′-cyclic thiophosphate promoting cleavage more than the *R*p 2′,3′-cyclic thiophosphate. The stereospecificity of sulfur effects on the equilibrium in $Co(NH_3)_6Cl_3$ buffer is consistent with evidence from cleavage and ligation rate measurements that nonbridging oxygens or sulfurs make stereospecific contacts in the active site that do not involve direct metal ion coordination. The absence of a detectable stereospecific thio effect in $MgCl_2$ and $MnCl_2$ buffers might result from differences among Mg^{2+}, Mn^{2+}, and $Co(NH_3)_6^{3+}$

Figure 5

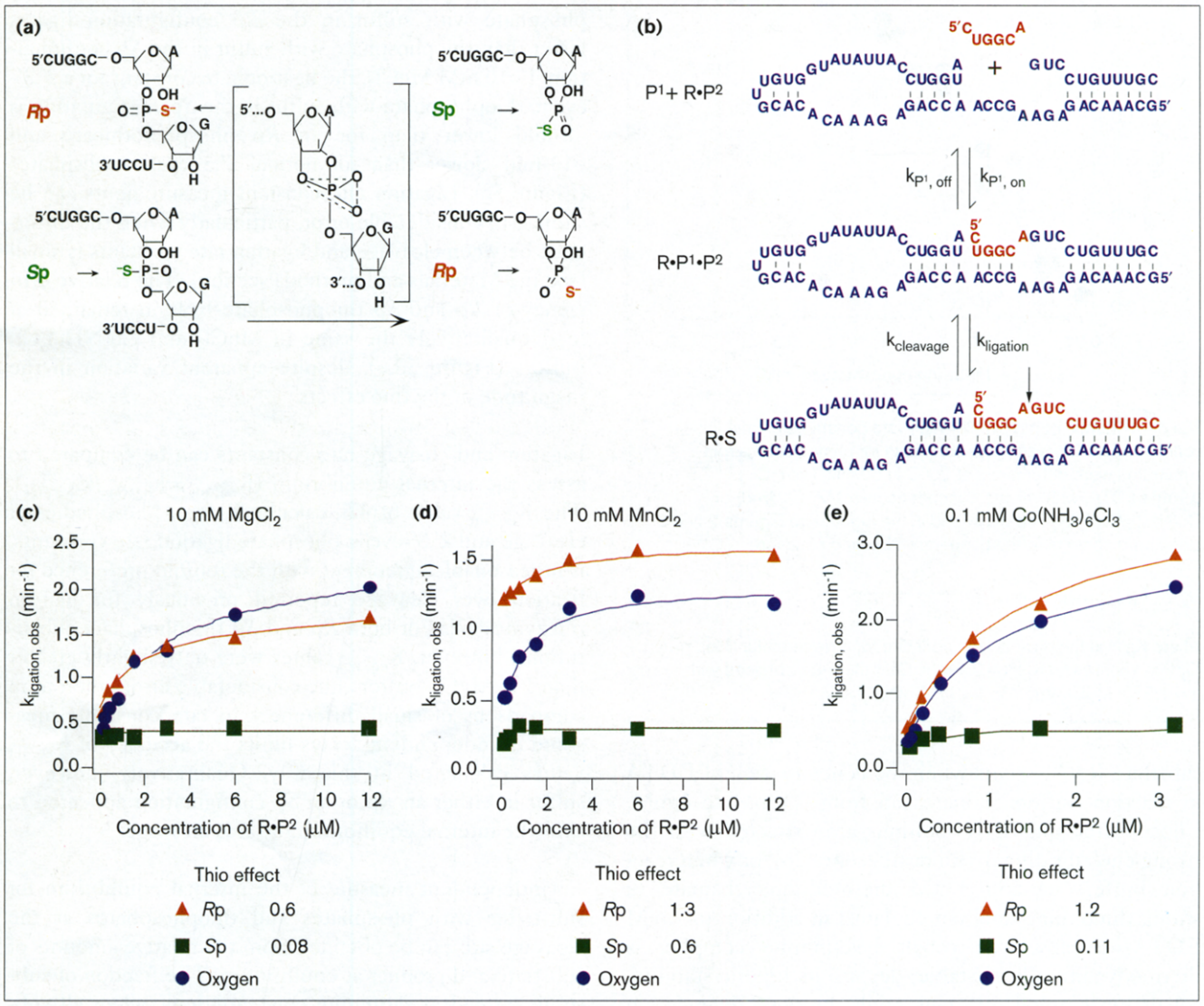

Analyzing the effects of sulfur substitutions of nonbridging oxygens on hairpin ribozyme ligation rate constants. **(a)** Ribozyme-mediated cleavage of 5′ ^{32}P-labeled substrates with sulfur substitutions in the *Rp* and *Sp* configurations yields 5′ products (P^1) with thiophosphate substitutions in the *Sp* and *Rp* configurations, respectively. **(b)** Sequences used for analysis of ligation kinetics. Trace amounts of 5′ ^{32}P-labeled P^1 (red) were combined with various excess concentrations of a binary complex containing the hairpin ribozyme and the 3′ cleavage product P^2 (blue), and the appearance of 5′ ^{32}P-labeled substrate was monitored over time. (The arrow indicates the position of cleavage.) Observed rates of ligation reflect the concentration of ternary complex containing the ribozyme and both cleavage products and the rate of the approach to the equilibrium between cleavage and ligation. Ligation rate constants of sulfur-substituted and unmodified products were determined at 25°C in 50 mM Tris-HCl, pH 7.5, 0.1 mM EDTA, with **(c)** 10 mM $MgCl_2$, **(d)** 10 mM $MnCl_2$, or **(e)** 0.1 mM $Co(NH_3)_6Cl_3$, by computing the best fit to:

$$k_{ligation,\ obs} = k_{ligation} \frac{[R \cdot P^2]}{[R \cdot P^2] + K_M{}^{P^1}} + k_{cleavage} \qquad (6)$$

Thio effect = $k_{ligation,\ S}$ / $k_{ligation,\ O}$, where $k_{ligation,\ S}$ and $K_{ligation,\ O}$ are ligation rates for sulfur and oxygen substituents, respectively.

counterions in their ability to stabilize R·S, R·P^1·P^2, and transition state structures.

Equilibrium dissociation constants (K_D) for P^1 binding to the R·P^2 binary complex can also be determined from the concentration dependence of ligation reaction extents (Table 2). $K_D{}^{P^1}$ values provide information about ground state interactions between P^1 and the R·P^2 binary complex. $K_M{}^S$ (Michaelis constant for substrate) and $K_M{}^{P^1}$ (Michaelis constant for P^1) values reveal little information about the effect of sulfur substitutions on ground state interactions because, in the hairpin ribozyme kinetic mechanism, K_M and K_D values are not necessarily equivalent [7]. $K_D{}^{P^1}$ values varied by about tenfold in reactions carried out in

Table 2

Ligation kinetics of normal and phosphorothioate-substituted RNAs.

	10 mM $MgCl_2$			10 mM $MnCl_2$			0.1 mM $Co(NH_3)_6Cl_3$		
Linkage	$k_{ligation}$ (min^{-1})	K_D^{P1} (μM)	$\frac{k_{ligation,\,S}}{k_{ligation,\,O}}$	$k_{ligation}$ (min^{-1})	K_D^{P1} (μM)	$\frac{k_{ligation,\,S}}{k_{ligation,\,O}}$	$k_{ligation}$ (min^{-1})	K_D^{P1} (μM)	$\frac{k_{ligation,\,S}}{k_{ligation,\,O}}$
Phosphate	2.0	2.1		0.41	0.38		2.8	0.26	
Rp phosphorothioate	1.2	1.7	0.6	0.55	0.84	1.2	3.4	0.42	1.2
Sp phosphorothioate	0.15	0.72	0.08	0.24	0.76	0.58	0.32	0.32	0.11

Abbreviations as in Table 1.

different buffers with the strongest P^1 binding observed in $Co(NH_3)_6Cl_3$ and the weakest P^1 binding observed in $MgCl_2$. Differences in K_D^{P1} values among different buffers are likely to reflect differences in the general effectiveness of Mg^{2+}, Mn^{2+} and $Co(NH_3)_6^{3+}$ counterions in promoting RNA structure. No significant differences were detected among K_D^{P1} values for P^1 RNAs with *Rp* or *Sp* phosphorothioates or normal phosphates in any buffer. Thus, sulfur substitutions had no detectable effects on ground state interactions within the $P^1{\cdot}R{\cdot}P^2$ ternary complex.

No intrinsic thio effect occurs in alkaline hydrolysis of RNA, an uncatalyzed reaction that occurs through the same chemical mechanism [28,29]. A difference in intrinsic reactivity between phosphates and phosphorothioates cannot, therefore, account for thio effects on hairpin cleavage. Furthermore, any intrinsic thio effect on cleavage chemistry is expected to be the same for both diastereomers [28,30], but *Rp* and *Sp* thio substitutions affect hairpin ribozyme cleavage rate constants differently. The stereospecificity of thio effects on hairpin cleavage indicates that *pro-Sp* and *pro-Rp* oxygens form different interactions within the hairpin active site, interactions that are more-or-less favorable when oxygen is replaced with sulfur. Because thio effects are not affected by the affinity of buffer cations for oxygen or sulfur, nonbridging oxygens or sulfurs must participate in distinct interactions with functional groups of the ribozyme, and not metal cations.

In an uncatalyzed reaction analogous to hairpin ribozyme-catalyzed ligation, alkaline hydrolysis of 2′,3′-cyclic phosphate does show an intrinsic thio effect (k_S/k_O) equal

Figure 6

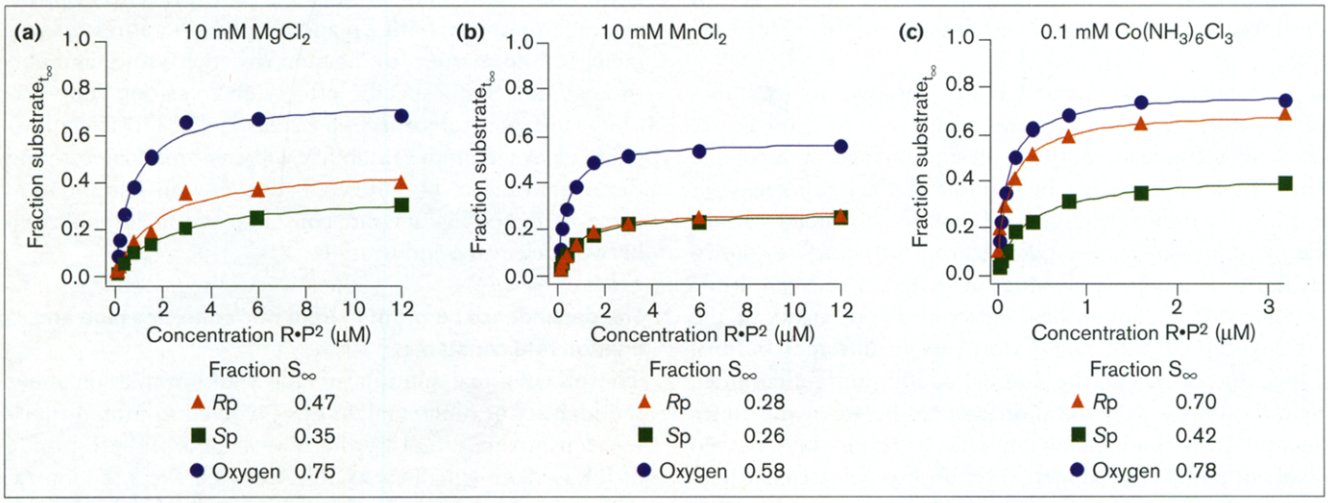

Analyzing the effects of sulfur substitutions of nonbridging oxygens on the internal equilibrium between cleavage and ligation. The fraction of 5′ ^{32}P-labeled P^1 converted to substrate by the end of ligation reactions (fraction $substrate_{t\infty}$) is plotted as a function of $R{\cdot}P^2$ concentration for ligation reactions carried out as described in Figure 5 with **(a)** 10 mM $MgCl_2$, **(b)** 10 mM $MnCl_2$, or **(c)** 0.1 mM $Co(NH_3)_6Cl_3$. The fraction of substrate at saturating concentrations of $R{\cdot}P^2$ (fraction S_∞) and K_D^{P1} values were computed from the fit to:

$$\text{fraction } S_\infty = K_{eq,\,int}\left[\frac{[R{\cdot}P^2]}{[R{\cdot}P^2]+K_D^{P1}}\right] \quad (7)$$

No correction was made for the fraction of 5′ ^{32}P-labeled P^1 (~15%) that remained unreactive. Consequently, fraction S_∞ is lower than $K_{eq,\,int}$ (the internal equilibrium, $k_{ligation}/k_{cleavage}$).

to 0.17 for both *Sp* and *Rp* diastereomers [30]. This intrinsic thio effect on 2′,3′-cyclic phosphate hydrolysis suggests that sulfur substitutions stabilize 2′,3′-cyclic phosphates relative to phosphorothiodiesters by ~1 kcal/mol, thereby raising the energy barrier for ligation. An intrinsic thio effect on hairpin ligation chemistry would be expected to reduce ligation rate constants for 2′,3′-cyclic thiophosphates and shift the internal equilibrium towards cleavage, as indeed the thio effects appear to do.

Although differences in stability between 2′,3′-cyclic thiophosphates and phosphates give rise to a chemical thio effect, interpretation of thio effects on hairpin ligation rate constants and the internal equilibrium is complicated by two factors. First, any intrinsic thio effect on ligation chemistry is superimposed over the stereospecific thio effects revealed by cleavage rate constant measurements that are independent of catalytic chemistry. Second, the hairpin ribozyme internal equilibrium is not determined exclusively by intrinsic chemical differences between substrates and products.

The balance between ribozyme-catalyzed ligation and cleavage is believed to reflect both an enthalpic contribution from the intrinsic chemistry of the reaction and an entropic contribution from differences in the dynamics of R·S and R·P^1·P^2 complexes that accompany catalysis [7,31]. Due to a small, ~1 kcal/mol, enthalpic advantage for 3′,5′-phosphodiesters relative to 2′,3′-cyclic phosphates [32], relief of strain in the 2′,3′-cyclic phosphate contributes a favorable enthalpy for ligation. Consistent with ligation rate and equilibrium measurements, sulfur substitutions are expected to counter the enthalpic advantage for diesters and shift the hairpin equilibrium towards cleavage.

If cleavage is accompanied by an increase in dynamics of the R·P^1·P^2 complex as the positions of P^1 and P^2 are no longer constrained by a diester linkage, a favorable enthalpy for ligation can be counteracted by an increase in entropy favoring cleavage [7,31]. Because metal cations vary in their ability to stabilize hairpin structures, as shown by the variation in K_D^{P1} values in buffers with Mg^{2+}, Mn^{2+} or $Co(NH_3)_6^{3+}$ counterions, entropic determinants of the internal equilibrium might well vary in different buffers. Thus, thio effects on the internal equilibrium reflect more than the intrinsic chemical differences between substrates and products, and metal ion effects cannot be assessed solely in terms of phosphate or phosphorothioate coordination. Sorting out the contribution of each factor is particularly difficult because the experimental evidence consists of small differences among rate and equilibrium constants.

A model consistent with the energetics of sulfur effects on hairpin-catalyzed cleavage and ligation is shown in Figure 7. Small, stereospecific thio effects on cleavage rate constants can be explained by specific interactions of

Figure 7

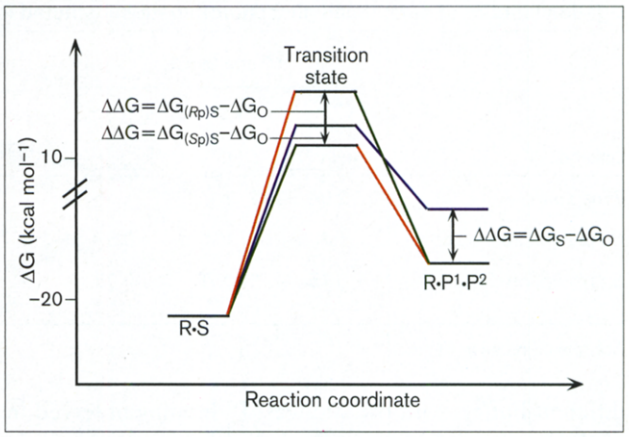

Free energy diagram representing the effects of sulfur substitutions on cleavage and ligation. The *Rp* and *Sp* phosphorothioates are proposed to raise or lower, respectively, the energy of the transition state based on stereospecific effects of sulfur substitutions on cleavage rate constants. An intrinsic difference in stability between 2′,3′-cyclic phosphates and phosphorothioates is proposed to reduce the free energy of cleavage products and increase the energy barrier for ligation equally for both diastereomers. The *Rp* or *Sp* configurations are indicated for cleavage substrates that give rise to cleavage products with the opposite configuration.

nonbridging oxygens within the active site that become more or less favorable when the *pro*-Sp or *pro*-Rp oxygens, respectively, are replaced with sulfur. Thus, an *Rp* phosphorothioate substitution raises the energy of the transition state, by ≤ 1 kcal/mol, while an *Sp* substitution reduces transition state energy by a smaller amount. If both thio diastereomers stabilize 2′,3′-cyclic phosphate cleavage products, both *Rp* and *Sp* phosphorothioates will increase the barrier to ligation by the same amount, ~1 kcal/mol. Stereospecific effects on transition state stability and nonstereospecific effects on 2′,3′-cyclic phosphate cleavage product stability will combine to determine the overall effect of sulfur substitutions on hairpin ribozyme-mediated ligation rate constants and the equilibrium between cleavage and ligation.

The dependence on pH of hairpin ribozyme cleavage and ligation rate constants

The pK_a of a reaction can provide vital information about the identity of functional groups involved in proton transfer steps, exemplified by the bell-shaped pH-rate profile of RNase A in which catalytic activity parallels the ionization state of histidine imidazoles [33]. The log-linear pH-rate profile for hammerhead cleavage appears to reflect the ionization state of metal-bound water implicating metal hydroxide as the general base catalyst [21].

In contrast, hairpin cleavage rate constants changed only 2.3-fold between pH 5.5 and pH 9 in $MgCl_2$ buffers (Figure 8a). With a pK_a value of 11.4 for the hydrated Mg^{2+}

ion [11], the concentration of $MgOH^-$ would increase 1000-fold across this pH range. Consequently, the absence of a corresponding increase in cleavage rate constants demonstrates that catalysis is not limited by the availability of $MgOH^-$ to serve as a general base catalyst.

Accuracy of cleavage rate constant measurements at pH values above 9 becomes limited in $MgCl_2$ buffers because of ribozyme and substrate RNA degradation due, presumably, to $MgOH^-$ mediated hydrolysis. Furthermore, sharp increases in K_M^S values at pH extremes, which are likely to be due to pH-dependent destabilization of intermolecular helices, make it difficult to approach saturating concentrations.

Virtually no background hydrolysis was detected in $Co(NH_3)_6Cl_3$ buffers, and K_M^S values remained in the experimentally accessible range at pH values as high as 10.1 (Figure 8b). The absence of detectable RNA hydrolysis in $Co(NH_3)_6Cl_3$ buffers at pH 10.1 provides strong evidence that the ability of $Co(NH_3)_6Cl_3$ to support catalysis does not reflect the presence of contaminants capable of forming metal hydroxides.

Hairpin cleavage and ligation rate constants changed less than fivefold between pH 4.9 and pH 10.1 (Figures 8a,9) in $Co(NH_3)_6Cl_3$ buffers. Stereospecific thio effects remained constant, arguing that cleavage rates monitor the step in the hairpin cleavage reaction that is also sensitive to sulfur substitutions throughout this pH range.

If a metal complex serves as general base catalyst and a step requiring proton transfer is rate determining, pH-rate profiles are expected to correlate with the ionization state of the catalyst. Thus, the shallow pH-dependence of hairpin cleavage and ligation rate constants in $MgCl_2$ and $Co(NH_3)_6Cl_3$ buffers indicates that hairpin catalysis is not limited by the availability of metal-bound hydroxide or any other metal complex acting as a general base catalyst.

Several explanations might account for the shallow pH dependence of hairpin catalysis. Buffer ions rather than metal ligands might serve as general base catalysts. Similar shallow pH-rate profiles were, however, determined at Tris buffer concentrations of 10–200 mM (data not shown). If general base catalysis is provided by buffer ions, and a step requiring proton transfer is limiting, cleavage rate constants would have increased with increasing buffer concentration.

Hairpin catalysis might be limited by a slow, pH-independent conformational change and not by the rate of the chemical step. The chemical step in the hairpin reaction might increase with pH in a log-linear fashion but acceleration of the chemical step could be hidden under a ceiling imposed by a slow conformational change. A rate-determining conformational step has been proposed to account for the pH-independence of *Tetrahymena* ribozyme-catalyzed cleavage at pH values above 7 [34]. But hairpin pH-rate profiles remain shallow with a variety of ribozyme and substrate sequences in self-cleaving and intermolecular configurations, at temperatures ranging from 25°C to 75°C, in buffers containing a variety of divalent metal cations, at an ionic strength as low as 0.01 mM $Co(NH_3)_6Cl_3$ and in 1 M urea (data not shown). In short, hairpin catalysis displays similar shallow pH-rate profiles under a variety of conditions that might be expected to accelerate any potentially rate-determining conformational change.

Figure 8

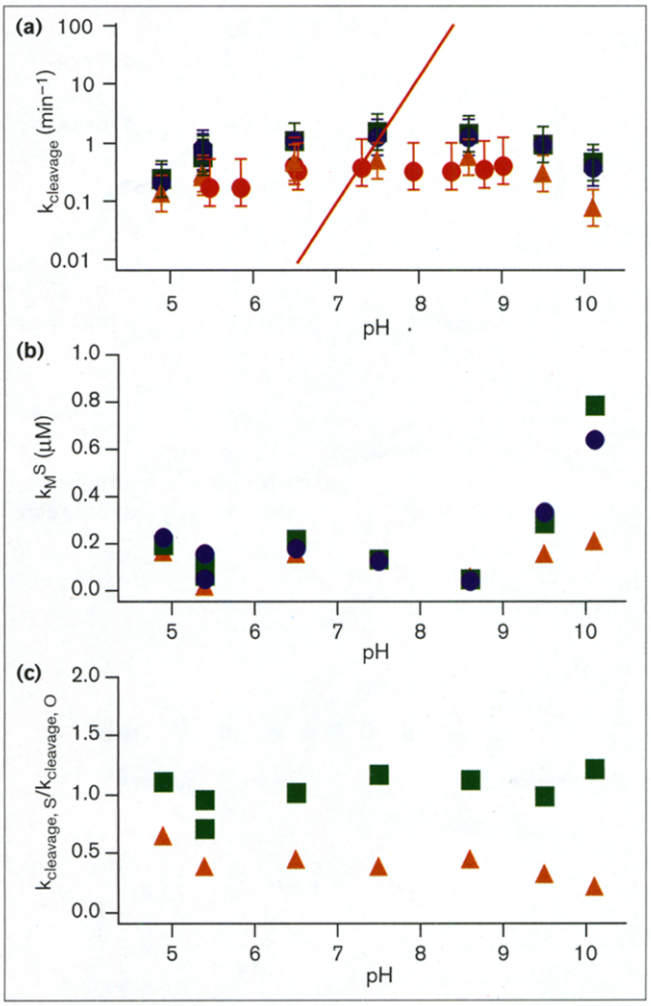

The pH dependence of hairpin ribozyme cleavage kinetics. **(a)** Cleavage rate constants, **(b)** K_M^S values, and **(c)** thio effects were determined for hairpin substrates with a normal phosphate (blue circle), an *Rp* phosphorothioate (orange triangle), or an *Sp* phosphorothioate (green square) at the cleavage site in 50 mM buffer, 0.25 mM $Co(NH_3)_6Cl_3$, 0.1 mM EDTA, at 25°C and for unmodified substrate (red circle) in 50 mM buffer, 10 mM $MgCl_2$, 0.1 mM EDTA (red circle), as described in the legends to Figures 2 and 3 except that the sequence of the substrate used for cleavage rate constant measurements in $MgCl_2$ buffer was 5′-CUGGCAGUCCUGUUU-3′. The red line represents a theoretical log-linear pH dependence.

Figure 9

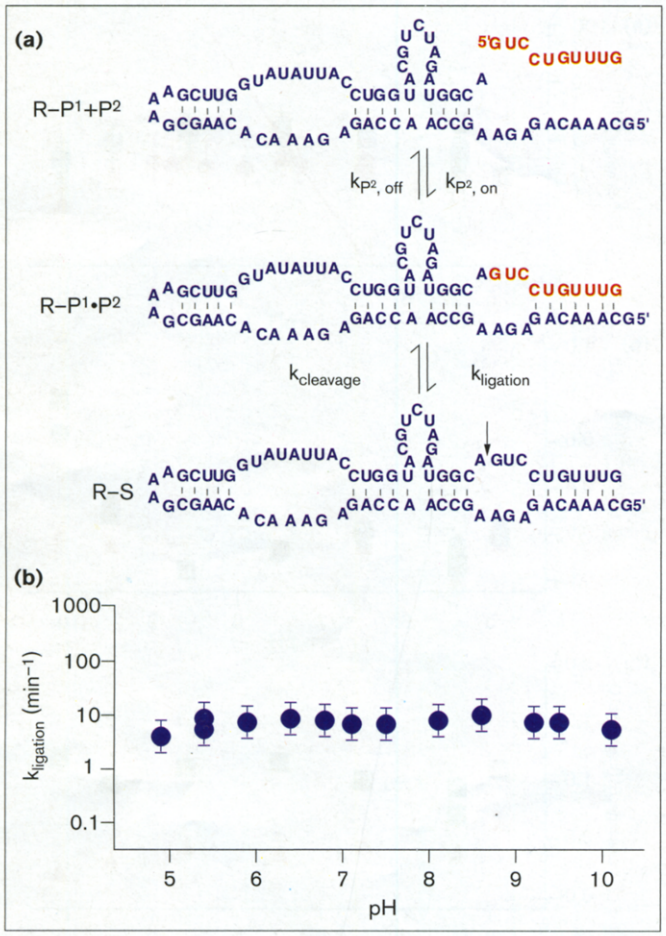

The pH dependence of hairpin ribozyme ligation kinetics. **(a)** Self-ligation kinetics were measured in 50 mM buffer, 0.25 mM $Co(NH_3)_6Cl_3$, 0.1 mM EDTA, at 25°C using a ribozyme configuration in which the P^1 RNA was covalently joined to the ribozyme through an oligonucleotide linker. Reactions contained a trace amount of uniformly labeled ribozyme and various concentrations of P^2 RNA. **(b)** Ligation rate constants were computed from the fit to:

$$k_{ligation,\,obs} = k_{ligation}\left[\frac{[R\cdot P^2]}{[R\cdot P^2]+K_M{}^{P^2}}\right] + k_{cleavage} \qquad (8)$$

If a log-linear dependence of hairpin catalytic chemistry is, in fact, masked by a slow conformational step, hairpin catalytic rate constants must be significantly faster than the hammerhead cleavage rate constant of 1 min^{-1} [27]. A hairpin cleavage rate constant greater than 0.2 min^{-1} at pH 5 would increase to > 200 min^{-1} at pH 8.

A rate-determining conformational change might be excluded if the thio effect on ligation rate constants could be shown to correspond with the intrinsic thio effect expected for nonenzymatic hydrolysis of 2′,3′-cyclic phosphates. Unfortunately, the superimposition of stereospecific thio effects on any intrinsic chemical thio effect and the error inherent in measuring small differences among rate constants precludes a conclusive interpretation of these data.

An alternative explanation for the shallow pH dependence is that cleavage and ligation rate constants monitor catalytic chemistry, but the highest barrier to catalysis is a pH-independent chemical step such as breaking the 5′ oxygen–phosphorus bond. Alternatively, bond making and bond breaking steps that require protonation and deprotonation could each be partially rate-determining. A complex, shallow pH-rate profile could result from a requirement for general acid and base catalysts with different pK_a values, perhaps provided by functional groups of the ribozyme. These possibilities remain to be tested.

Significance

Hairpin ribozymes (RNA enzymes) catalyze the same chemical reaction as ribonuclease A and yet RNAs do not usually have functional groups analogous to the catalytically essential histidine and lysine sidechains of protein ribonucleases. Some RNA enzymes appear to recruit metal ions to act as Lewis acids in charge stabilization and metal-bound hydroxide for general base catalysis. Prompted by reports that the hairpin ribozyme functions in the presence of metal ion chelators, we investigated whether the hairpin ribozyme exploits a metal-ion-independent strategy.

Small, stereospecific effects of thiophosphate substitutions on hairpin-ribozyme-catalyzed cleavage and ligation and the ability of cobalt hexammine to support hairpin catalysis indicate that the rate-determining step in hairpin-ribozyme-catalyzed cleavage and ligation does not depend on direct coordination to metal cations. Furthermore, the shallow pH dependence of hairpin catalysis in $MgCl_2$ and $Co(NH_3)_6Cl_3$ buffers shows that the rate-determining step does not depend on metal-bound hydroxide acting as a general base catalyst. Several models might account for the unusual pH independence and metal-ion-independence of hairpin catalysis. Hairpin cleavage and ligation might be limited by a slow conformational change. A pH independent and metal-cation-independent chemical step, such as breaking the 5′ oxygen–phosphorus bond, might be rate determining. Finally, functional groups within the ribozyme might participate directly in catalytic chemistry. Whichever the case, the hairpin ribozyme appears to employ unique strategy for RNA catalysis.

Materials and methods

Preparation of RNAs

Unmodified ribozyme, substrate and 3′ cleavage product RNAs were prepared and labeled with ^{32}P as previously described ([7], and references therein). Briefly, ribozyme RNAs were synthesized by T7 RNA polymerase transcription of partially duplex synthetic DNA templates and purified by denaturing gel electrophoresis. Cleavage substrates

and 3′ cleavage products (3′ ligation substrates) were synthesized chemically, deprotected, desalted and gel purified. 5′ ^{32}P-labeled substrate RNAs were prepared by reaction with T4 polynucleotide kinase and [γ-^{32}P] ATP and [α-^{32}P] ribozyme RNAs were prepared by *in vitro* transcription with [α-^{32}P] ATP. RNA concentrations were determined by assuming a residue extinction coefficient of $6.6 \times 10^3\,M^{-1}\,cm^{-1}$ at 260 nm or calculated from the specific activity of the [γ-^{32}P] ATP or [α-^{32}P] ATP used for labeling.

Substrate RNAs with sulfur substitutions were synthesized using conventional phosphoramidite chemistry except that reaction with 3H-1,2-benzodithiol-3-one, 1,1-dioxide (Beaucage reagent) replaced standard iodine oxidation of the diester linkage corresponding to the reactive phosphorus [20]. After deprotection and desalting, the mixture of *Rp* and *Sp* thio-substituted RNAs were fractionated by reverse phase HPLC (semi-preparative C18 column, Microsorb MV, Rainin; Gait, 1992), using a gradient of 2–4.5% acetonitrile in 0.1 M ammonium acetate. 5′ cleavage products (5′ ligation substrates) were prepared through ribozyme-mediated cleavage of 5′ ^{32}P-labeled substrates, fractionated by denaturing gel electrophoresis, eluted and desalted by G15 Sephadex chromatography in water. Because cleavage occurs with inversion of configuration [35], the *Rp* thio-substituted substrate yields a 5′ cleavage product with an *Sp* thio 2′,3′-cyclic phosphate (*endo*) and *Sp* thio-substituted substrate yields a 5′ cleavage product with an *Rp* thio 2′,3′-cyclic phosphate (*exo*).

The location of phosphorothioate linkages in RNA from each C18 fraction was confirmed by I_2 cleavage [36]. The *Rp* and *Sp* diastereomers were assigned through partial digestion of 5′ ^{32}P-labeled labeled RNA from each C18 fraction and unmodified RNA with stereospecific nucleases. In reactions with P^1 endonuclease, which cannot cleave an *Rp* phosphorothioate linkage [37], the thioester linkage of RNA from the early C18 fraction resisted cleavage through 20 min incubation with 5 ng/ml nuclease P^1, 300 mM sodium acetate pH 5.3, 0.2 mg/ml carrier RNA, 0.1 mM EDTA, at 25°C. RNA from the late C18 fraction showed evidence of some cleavage at the phosphorothioate linkage under the same conditions, but far less cleavage than observed for the corresponding phosphodiester linkage in unmodified RNA. In reactions with snake venom phosphodiesterase, which favors cleavage of the *Rp* phosphorothioate [28], the fragment corresponding to cleavage of the phosphorothioate linkage in RNA from the late C18 fraction was approximately twofold less abundant than the corresponding fragment in reactions with RNA from the early C18 fraction after digestion with 20 ng/ml snake venom phosphodiesterase in 50 mM Tris-HCl, pH 7.5, 10 mM $MgCl_2$, 0.2 mg/ml carrier RNA, 0.1 mM EDTA, at 25°C. Thus, RNA from the early C18 fraction was inferred to contain sulfur in the *Rp* configuration and RNA from the late C18 fraction was inferred to contain sulfur in the *Sp* configuration.

Ribozyme-mediated cleavage of normal and sulfur-substituted substrates generated 5′ products that co-migrated during denaturing gel electrophoresis, demonstrating that cleavage occurs precisely at the phosphorothioate linkage. The *Rp* and *Sp* sulfur-substituted substrates cleaved almost completely and reaction kinetics remained linear through at least three half lives, evidence that substrate RNA preparations were chemically homogeneous.

Kinetics analyses

Unless otherwise indicated, cleavage and ligation reactions were carried out in 50 mM Tris-HCl, 0.1 mM EDTA, and the indicated metal ions at pH 7.5 and 25°C, as previously described [7], except that substrate and product RNAs were not subjected to a heat denaturation step to avoid degradation of the phosphorothioate linkage. Separate solutions of ribozyme, substrate and product RNAs were equilibrated in buffer at 25°C for ≥ 10 min and reactions were initiated by mixing ribozyme with substrate or product RNAs. Samples were removed at intervals, quenched with an equal volume or more of 8 M urea, 25 mM EDTA, 0.002% bromophenol blue, 0.002% xylene cyanol, and fractionated on denaturing gels. Radioactivity in product and substrate bands was quantitated by radioanalytic scanning.

To maximize accuracy in measuring small differences in reaction kinetics among modified and unmodified RNAs, a single solution of ribozyme was divided among each solution of substrate or product RNA in parallel kinetics time courses.

Kinetic parameters for substrate cleavage were determined from single turnover reactions with various ribozyme concentrations in excess of trace amounts of 5′ ^{32}P-labeled substrate or product RNAs as previously described [7]. Observed cleavage rates were obtained from fits to:

$$\text{fraction product} = e^{-k_{obs}t} \quad \text{or} \quad -k_{obs}t = \ln(\text{fraction S}) \qquad (1)$$

after normalization to the fraction of substrate that remained intact at the end of the reaction, which was > 0.9 or 0.8 for sulfur-substituted and unmodified substrates, respectively. Plots of $k_{cleavage,\,obs}$ versus $k_{cleavage,\,obs}/[R]$ (where [R] is the ribozyme concentration) were used to calculate K_M^S values from the slope and cleavage rate constants, $k_{cleavage}$, from the y-intercept. Kinetic parameters obtained from similar cleavage experiments carried out at different times varied no more than twofold while the ratio of values obtained among modified and unmodified substrates within a single experiment varied < 30%.

Ligation rate constants for sulfur-substituted and unmodified 5′ cleavage product (P^1) RNAs were measured in reactions with trace amounts of ^{32}P-labeled 5′ product (P^1) and various concentrations of a binary complex containing the ribozyme bound to 3′ cleavage product (R·P^2), as previously described [7]. Observed ligation rates and the fraction of substrate at equilibrium were determined from exponential fits of fraction S versus time. Because substrate formed through ligation remains associated with the ribozyme, the observed ligation rate reflects the approach to equilibrium between cleavage and ligation and is the sum of cleavage and ligation rates. Ligation rate constants were obtained by computing the fit to:

$$k_{obs,\,ligation} = k_{ligation}\left[\frac{[R\cdot P^2]}{[R\cdot P^2]+K_M{}^{P^2}}\right] + k_{cleavage} \qquad (2)$$

where [R·P^2] (concentration of R·P^2) is assumed to equal $[R]_{total}$ (total concentration of R). The accuracy of ligation kinetics parameters determined for sulfur-substituted RNAs was limited because observed ligation rates varied approximately twofold between saturating and subsaturating concentrations of R·P2. Values of $k_{ligation}$ determined for sulfur-substituted RNAs varied as much as fivefold among independent experiments while the ratio of values obtained among modified and unmodified substrates within a single experiment varied < 50%.

To assess the effect of phosphorothioate substitutions on the internal equilibrium between cleavage and ligation ($K_{eq,\,int} = k_{ligation}/k_{cleavage}$), the final fraction of product converted to substrate was measured at the end of reactions with trace amounts of ^{32}P-labeled 5′ product (P^1) and various concentrations of a binary complex containing the ribozyme bound to 3′ cleavage product (R·P^2). The fraction of product converted to substrate by the end of a ligation reaction is the product of $K_{eq,\,int}$ and the amount of P^1 associated with R·P^2 binary complex, or [R·P^2]/([R·P^2] + $K_D{}^{P^2}$). $K_D{}^{P^1}$ and the fraction of substrate with saturating concentrations of R·P^2 at equilibrium were determined by computing the fit to:

$$\text{fraction } S_\infty = K_{eq,\,int}\left[\frac{[R\cdot P^2]}{[R\cdot P^2]+K_D{}^{P^1}}\right] \qquad (3)$$

At the high concentrations used for ligation experiments ~15% of P^1 RNA fails to react, probably due to nonproductive complex formation [7], resulting in an underestimation of $K_{eq,\,int}$. Consequently, reported values for the fraction of substrate at equilibrium are lower than $K_{eq,\,int}$.

In experiments to determine the pH dependence of hairpin ribozyme ligation with unmodified RNAs, self-ligation kinetics were measured in reactions with a trace amount of ^{32}P-labeled ribozyme and various

excess concentrations of 3′ cleavage product (P^2) RNA. $k_{ligation}$ was computed from the fit to:

$$k_{ligation,\,obs} = k_{ligation}\left[\frac{[P^2]}{[P^2]+K_M{}^{P^2}}\right] + k_{cleavage} \quad (4)$$

The pH dependence of cleavage and ligation rate constants was measured in 0.1 mM EDTA with 0.25 mM $Co(NH_3)_6Cl_3$ or 10 mM $MgCl_2$, as indicated, and the following buffers at a concentration of 50 mM: Na acetate, pH 4.9–5.4; Na MES (2-[N-morpholino]ethanesulfonic acid), pHs 5.4, 5.9, 6.5, and 6.8; Na PIPES (piperazine-N,N′-bis[2-ethanesulfonic acid]), pH 6.4; Tris-HCl, pHs 7.1, 7.3, 7.5, 8.1, 8.4, 8.6, and 8.8; and Na CHES (2-[N-cyclohexylamino]ethanesulfonic acid), pHs 9.0, 9.2, 9.5, and 10.1; with pH values measured at 25°C. The RNA sequences used for measurement of kinetic parameters in $Co(NH_3)_6Cl_3$ are shown in Figures 2a and 9. The sequence of the substrate RNA used to determine cleavage rate constants in $MgCl_2$ buffer was 5′-CUGGCAGUCCUGUUU-3′.

To avoid formation of insoluble metal oxides [21], buffers and RNA solutions were prepared immediately before use. To minimize exchange of amine ligands of Co^{3+} in $Co(NH_3)_6Cl_3$, stock solutions were stored at −20°C and protected from exposure to light.

Acknowledgements

We thank Heidi Erlacher for help in fractionating phosphorothioate diastereomers. This work was supported by NIH grant GM 46422. LAH was the recipient of a National Research Service Award from the National Institute of General Medical Sciences.

References

1. Long, D.M. & Uhlenbeck, O.C. (1993). Self-cleaving catalytic RNA. *FASEB J.* **7**, 25-30.
2. Scott, W.G. & Klug, A. (1996). Ribozymes: structure and mechanism in RNA catalysis. *Trends Biochem. Sci.* **21**, 220-224.
3. Buzayan, J.M., Gerlach, W.L. & Bruening, G. (1986). Nonenzymatic cleavage and ligation of RNAs complementary to a plant virus satellite RNA. *Nature* **323**, 349-353.
4. Hampel. A. & Tritz, R. (1989). RNA catalytic properties of the minimum (−)sTRSV sequence. *Biochemistry* **28**, 4929-4933.
5. Burke, J.M., Butcher, S.E. & Sargueil, B. (1996). Structural analysis and modifications of the hairpin ribozyme. In *Catalytic RNA*. (Eckstein, F. & Lilley, D.M.J., eds), pp. 129-143, Springer-Verlag, Berlin, Germany.
6. Feldstein, P.A. & Bruening, G. (1993). Catalytically active geometry in the reversible circularization of 'mini-monomer' RNAs derived from the complementary strand of tobacco ringspot virus satellite RNA. *Nucleic Acids Res.* **21**, 1991-1998.
7. Hegg, L.A. & Fedor, M.J. (1995). Kinetics and thermodynamics of intermolecular catalysis by hairpin ribozymes. *Biochemistry* **34**, 15813-15828.
8. Welch, P.J., Hampel, A., Barber, J., Wong-Staal, F. & Yu, M. (1996). Inhibition of HIV replication by the hairpin ribozyme. In *Catalytic RNA*. (Eckstein, F. & Lilley, D.M.J., eds), pp. 315-327, Springer-Verlag, Berlin, Germany.
9. Richards, F.M. & Wycoff, H.W. (1971). Bovine pancreatic ribonuclease. In *The Enzymes*, Vol. 4, (Boyer, P.D., ed.), pp. 647-806, Academic Press, New York.
10. Nishikawa, S., *et al.*, & Ikehara, M. (1987). Two histidine residues are essential for ribonuclease T1 activity as is the case for ribonuclease A. *Biochemistry* **26**, 8620-8624.
11. Pan, T., Long, D.M. & Uhlenbeck, O.C. (1993). Divalent metal ions in RNA folding and catalysis. In *The RNA World*. (Gesteland, R.F. & Atkins, J.F., eds), pp. 271-302, Cold Spring Harbor Laboratory Press, Cold Spring Harbor, New York.
12. Yarus, M. (1993). How many catalytic RNAs? Ions and the Cheshire cat conjecture. *FASEB J.* **7**, 31-39.
13. Pyle A.M. (1993). Ribozymes: a distinct class of metalloenzymes. *Science* **261**, 709-714.
14. Steitz, T.A. & Steitz, J.A. (1993). A general two-metal-ion mechanism for catalytic RNA. *Proc. Natl Acad. Sci. USA* **90**, 6498-6502.
15. Dahm, S.C. & Uhlenbeck, O.C. (1991). Role of divalent metal ions in the hammerhead RNA cleavage reaction. *Biochemistry* **30**, 9464-9469.
16. Piccirilli, J.A., Vyle, J.S., Caruthers, M.H. & Cech, T.R. (1993). Metal ion catalysis in the *Tetrahymena* ribozyme reaction. *Nature* **361**, 85-88.
17. Jaffe, E.K. & Cohn, M. (1979). Diastereomers of the nucleoside phosphorothioates as probes of the structure of metal nucleotide substrates and of the nucleotide binding site of yeast hexokinase. *J. Biol. Chem.* **254**, 10839-10845.
18. Pecoraro, V.L., Hermes, J.D. & Cleland, W.W. (1984). Stability constants of Mg^{2+} and Cd^{2+} complexes of adenine nucleotides and thionucleotides and rate constants for formation and dissociation of MgATP and MgADP. *Biochemistry* **23**, 5262-5271.
19. Koizumi, M. & Ohtsuka, E. (1991). Effects of phosphorothioate and 2 amino groups in hammerhead ribozymes on cleavage rates and Mg^{2+} binding. *Biochemistry* **30**, 5145-5150.
20. Slim, G. & Gait, M.J. (1991). Configurationally defined phosphorothioate-containing oligoribonucleotides in the study of the mechanism of cleavage of hammerhead ribozymes. *Nucleic Acids Res.* **19**, 1183-1188.
21. Dahm, S.C., Derrick, W.B. & Uhlenbeck, O.C. (1993). Evidence for the role of solvated metal hydroxide in the hammerhead cleavage mechanism. *Biochemistry* **32**, 13040-13045.
22. Forster, A.C., Jeffries, A.C., Sheldon, C.C. & Symons, R.H. (1987). Structural and ionic requirements for self-cleavage of virusoid RNAs and trans self-cleavage of viroid RNA. *Cold Spring Harbor Symp. Quant. Biol.* **52**, 249-259.
23. Chowrira, B.M. & Burke, J.M. (1991). Binding and cleavage of nucleic acids by the 'hairpin' ribozyme. *Biochemistry* **30**, 8518-8522.
24. Buzayan, J.M., Feldstein, P.A., Bruening, G. & Eckstein, F. (1988). RNA mediated formation of a phosphorothioate diester bond. *Biochem. Biophys. Res. Commun.* **156**, 340-347.
25. Lippard, S.J. & Berg, J.M. (1994). *Principles of Bioinorganic Chemistry*. University Science Books, Mill Valley, California, USA.
26. Holmquist, B. (1988). Elimination of adventitious metals. *Methods Enzymol.* **158**, 6-12.
27. Fedor, M.J. & Uhlenbeck, O.C. (1992). Kinetics of intermolecular cleavage by hammerhead ribozymes. *Biochemistry* **31**, 12042-12054.
28. Burgers, P.M.J. & Eckstein, F. (1979). Diastereomers of 5′-O-adenosyl 3′-O-uridyl phosphorothioate: chemical synthesis and enzymatic properties. *Biochemistry* **18**, 592-596.
29. Herschlag, D., Piccirilli, J.A. & Cech, T.R. (1991). Ribozyme-catalyzed and nonenzymatic reactions of phosphate diester: rate effects upon substitution of sulfur for a nonbridging phosphoryl oxygen atom. *Biochemistry* **30**, 4844-4854.
30. Eckstein, F. (1968). Uridine 2′,3′-*O,O*-cyclophosphorothioate as substrate for pancreatic ribonuclease (I) *FEBS Lett.* **2**, 85-86.
31. Hertel, K.J., Herschlag, D. & Uhlenbeck, O.C. (1994). A kinetic and thermodynamic framework for the hammerhead ribozyme reaction. *Biochemistry* **33**, 3374-3385.
32. Gerlt, J.A., Westheimer, F.H. & Sturtevant, J.M. (1975). The enthalpies of hydrolysis of acyclic, monocyclic, and glycoside cyclic phosphate diesters. *J. Biol. Chem.* **250**, 5059-5067.
33. del Rosario, E.J. & Hammes, G.G. (1969). Kinetic and equilibrium studies of the ribonuclease-catalyzed hydrolysis of uridine 2′,3′-cyclic phosphate. *Biochemistry* **8**, 1884-1895.
34. Herschlag, D. & Khosla, M. (1994). Comparison of pH dependencies of the Tetrahymena ribozyme reactions with RNA 2′-substituted and phosphorothioate substrates reveals a rate-limiting conformational step. *Biochemistry* **33**, 5291-5297.
35. van Tol, H., Buzayan, J.M., Feldstein, P.A., Eckstein, F. & Bruening, G. (1990). Two autolytic processing reactions of a satellite RNA proceed with inversion of configuration. *Nucleic Acids Res.* **18**, 1971-1975.
36. Schatz, D., Leberman, R. & Eckstein, F. (1991). Interaction of Escherichia coli tRNA(Ser) with its cognate aminoacyl-tRNA synthetase as determined by footprinting with phosphorothioate-containing tRNA transcripts. *Proc. Natl Acad. Sci. USA* **88**, 6132-6136.
37. Potter, B.V.L., Conolly, B.A. & Eckstein, F. (1983). Synthesis and configurational analysis of a dinucleoside phosphate isotopically chiral at phosphorus. Stereochemical course of Penicillium citrum nuclease P1 reaction. *Biochemistry* **22**, 1369-1377.